Geological Quarterly, 2007, **51** (2): 127–146

Geochemical composition of Vistulian loess and micromorphology of interstadial palaeosols at the Kolodiiv site (East Carpathian Foreland, Ukraine)

Bożena ŁĄCKA, Maria ŁANCZONT, Teresa MADEYSKA and Andrij BOGUCKYJ

Łącka B., Łanczont M., Madeyska T. and Boguckyj A. (2007) — Geochemical composition of Vistulian loess and micromorphology of interstadial palaeosols at the Kolodiiv site (East Carpathian Foreland, Ukraine). Geol. Quart., **51** (2): 127–146. Warszawa.

This paper summarizes geochemical and palaeopedological investigations of the Upper Pleistocene loess-palaeosol sequences at the Kolodiiv site. The Kolodiiv 2, 3 and 5 profiles were selected for this study. The Kolodiiv 2 profile contains loesses, interglacial (Eemian) and interstadial (Vistulian) palaeosols. A set of Early Vistulian soils overlying Eemian gyttja and peat is exposed in the Kolodiiv 3 and 5 profiles. The mineral composition of the 50–2 μm silt fraction was analysed using non-oriented powder samples by means of X-ray diffraction. The total concentrations of nine major (Si, Ti, Al, Fe, Mn, Mg, Ca, K and Na) and nine trace elements (Zn, Pb, Ni, Rb, Cr, Sr, Ba, Co, V) as well as the humus content and loss on ignition were measured. The major elements concentrations in mineral deposits from the Kolodiiv 2 loess-palaeosol sequence indicate that the loess particles were derived from poorly weathered source rocks that have undergone at least one sedimentary cycle. Climatic conditions have strongly influenced the mobilization and accumulation of elements in the palaeosol horizons due to the changes in the intensity of weathering and pedogenic processes. For the micromorphological study, ten samples from the Kolodiiv 3 and 5 profiles were used. Thin sections representing the Kolodiiv and Dubno set of palaeosols from Early Vistulian and Middle Pleniglacial show, besides palaeopedologic characteristics, significant evidence of redeposition of sediments and soils.

Bożena Łącka, Teresa Madeyska, Institute of Geological Sciences, Polish Academy of Sciences, Twarda 51/55, PL-00-818 Warszawa, Poland, e-mails: lacka@twarda.pan.pl, tmadeysk@twarda.pan.pl; Maria Łanczont, Department of Physical Geography and Palaeogeography, Maria Curie-Skłodowska University, al. Kraśnicka 2 CD, PL-20-718 Lublin, Poland, e-mail: lanczont@biotop.umcs.lublin.pl; Andrij Boguckyj, Department of Geography, Lvov University, Doroshenka 41, 790000 Lvov, Ukraine *(received: March 3, 2006; accepted: January 17, 2007).*

Key words: Ukraine, Late Pleistocene, palaeosols, loess, micromorphology, geochemistry.

INTRODUCTION

The Kolodiiv set of loess-palaeosol profiles is situated on the right bank of the Sivka River, near its confluence with the Dniester River (Fig. 1). The description of these and of their geological and geomorphological settings are given by Łanczont and Boguckyj (2002, 2007). The preliminary investigation results have already been published together with those obtained for other profiles from the Halyč Region (Madeyska, 2002) and in this volume.

The Kolodiiv 2, 3 and 5 profiles were selected for geochemical and palaeopedological study. The Kolodiiv 2 profile is located in the eastern part of the site and contains loess deposits and palaeosols of the Eemian Interglacial and of the Vistulian Glacial, overlying river sands. A set of Early Vistulian soils overlying Eemian gyttja, together with palaeosols that form interstadials of Interplenivistulian occur in the Kolodiiv 3 profile, situated in the central part of the exposure. In the Kolodiiv 5 profile, situated in the western part of the exposure, these soils overlie Eemian peat. The Early Vistulian palaeosols are characterized by great spatial variability.

DESCRIPTION OF THE PROFILES

The Kolodiiv 2 profile was examined several times in 1999, 2001 and 2003. Most samples for palaeomagnetic investigations (Nawrocki *et al*., 2007) were taken in 1999, but additional samples for these analyses and samples for TL dating were taken in 2001. The profile description herein was made in 2003 when it was sampled for grain size (Frankowski *et al*., 2007) and for geochemical analyses. Some differences were found in the deposit sequence, thickness and characteristics of individual layers in comparison with descriptions made earlier (in 1999 and 2001). These differences were mainly the results of

local variability of sedimentation and denudation processes. Based on that comparison, it can be concluded that the past microrelief was varied.

Lithological terminology after Polish standard (PN–86/B–02480) is used in the description and colours were described using Munsell Soil Color Charts.

The **Kolodiiv 2 profile** (Fig. 2):

0–1.8 m. Holocene soil:
- — Humus horizon 0.4 m thick, medium silt, dark brown (7.5 YR4/2 after Munsell..., 1954), macroporous and porous, with iron-manganese concretions; HCl (–). Distinct lower boundary visible as colour change.
- — Eluvial horizon (Eet) 0.1 m thick, loose sandy silt, pale grey with brown tint, of platy structure (plates up to 5 mm thick), macroporous, with very numerous iron-manganese concretions; HCl (–). Distinct lower boundary visible as colour and structure change. Material of this horizon penetrates the underlying deposit to a depth of 50 cm along vertical fissures and small interstices between soil aggregates.
- — Horizon Bt 1.3 m thick, compact, macroporous loamy silt, reddish brown (7.5 YR5/4), with prismatic structure well developed in the upper part and weaker in the bottom part where the deposit is more homogeneous, with dark iron-manganese concretions and other concentrations of iron compounds (Liesegang rings). Single mole tunnels were found; HCl (–). Gradual transition to the underlying layer.

1.8–4.4 m. Loess, coarse silt, brown (10 YR4/3), rather homogeneous, HCl (+). Distinct lower boundary.

4.4–5.1 m. Sandy silt, gleyed, distinctly stratified, deformed by solifluction, with manganese spots, HCl (+). Distinct lower boundary.

5.1–8.3 m. Dubno 1 set of palaeosols, set of several interstadial palaeosols of brown gleyed and gley type, with total thickness of 3.2 m:
- — 5.1–5.9 m. Set of two thin soils composed of two silty loam horizons: A — greyish brown (2.5 YR5/2) and B — brown (10 YR4/2).
- — 5.9–6.3 m. Palaeosol composed of gleyed A and B horizons.
- — 6.3–7.3 m. Palaeosol composed of gleyed A horizon 0.4 m thick, dark yellowish brown: 10 YR4/4 and B horizon 0.6 m thick, strong brown (7.5 YR5/4) silty loam, enriched in iron compounds. Distinct erosion boundary between these horizons.
- — 7.3–8.3 m. Palaeosol composed of A horizon — gleyed, dark greyish brown (10 YR4/2) silty loam, 0.6 m thick, with undulose hardpan 1–2 cm thick, and B horizon — dark reddish brown (7.5 YR4/4) silty loam, 0.4 m thick, strongly enriched in iron compounds, with casts of not fully reticulate structure of ground ice, and with sharp lower boundary.

8.3–9.3 m. Coarse and medium silt, dark brown (10 YR4/3).

9.3–11.2 m. Stratified deluvial coarse and medium silt and silty loam, dark yellowish brown (10 YR4/3) and dark brown (7.5 YR4/2), in the bottom part (0.3 m) — sandy silt.

11.2–11.9 m. Sandy silt and silty loam, stratified, deformed by solifluction, yellowish brown (10 YR5/4).

11.9–12.6 m. The Dubno 2 palaeosol. Ag horizon 0.3 m thick, greyish brown (10 YR5/2) silty loam. B horizon 0.4 m thick, dark brown (7.5 YR4/2) silty loam. Lower boundary sharp, sinuous, of erosion origin.

12.6–13.3 m. Solifluction layer, stratified sandy silt, dark brown (10 YR4/3). Lower boundary sharp, of erosional origin.

13.3–19.1 m. Horohiv (Eemian–Early Vistulian) set of palaeosols composed of three interstadial soils (Kolodiiv 1, Kolodiiv 2 and Kolodiiv 3) and two Eemian soils (I — younger and II — older):
- — 13.3–13.6 m. Early Vistulian palaeosol Kolodiiv 1, truncated. Horizon B, dark brown (7.5 YR4/3) silty loam. Lower boundary sharp, sinuous.
- — 13.6–15.0 m. Early Vistulian palaeosol Kolodiiv 2. Humus horizon 0.8 m thick, strongly gleyed, dark brown (10 YR4/3) silty loam, pale grey in the bottom part. Horizon B 0.6 m thick, dark yellowish brown (10 YR4/4) silty loam, developed on solifluction deposits over the Kolodiiv 3 soil. Distinct lower boundary, sinuous.
- — 15.0–15.7 m. Early Vistulian palaeosol Kolodiiv 3. Humus horizon, stratified silty loam, very dark brown (7.5 YR3/2). Deposit is strongly deformed, with traces of redeposition along fossil slope. Agglomerations of charcoals up to 3 cm in diameter occur in the upper part of the layer. Distinct lower boundary.
- — 15.7–16.5 m. Younger Eemian palaeosol (I). Horizon Eet of the interglacial forest soil, 0.2 m thick, typically developed, pale grey. Horizon B of the interglacial forest soil, 0.6 m thick, dark brown (10 YR4/3) silty loam, darker in the bottom part where it is developed on the material of A the horizon of the underlying soil of the Horohiv soil. Lower boundary uneven.
- — 165.5–19.1 m. Older Eemian palaeosol (II). Horizon A 0.2 m thick, strongly disturbed, only its redeposited remnants are preserved as coarse silt, dark greyish brown (7.5 YR4/2). Horizon Eet with 0.7 m thick, coarse silt, pale brown (10 YR5/3) of platy structure, with very numerous iron-manganese concretions and casts of zoogenic structures associated with the existence of a small pedofauna. Gradual transition. Horizon B with variable thickness of 1.1–1.5 m, coarse silt and loamy silt, distinctly stratified in the lower part, dark reddish brown (7.5 YR4/4), gleyed. Different forms of iron-manganese concentrations are developed within the horizon, i.e. small concretions up to 3 mm in diameter, and Liesegang rings up to 4 cm in diameter. Many faunal tube casts filled with material from the eluvial horizon are visible as pale spots. Distinct lower boundary.

19.1–19.2 m. Stratified sands.

The description of the Kolodiiv 5 profile and the main analytical results were published by Łanczont and Boguckyj

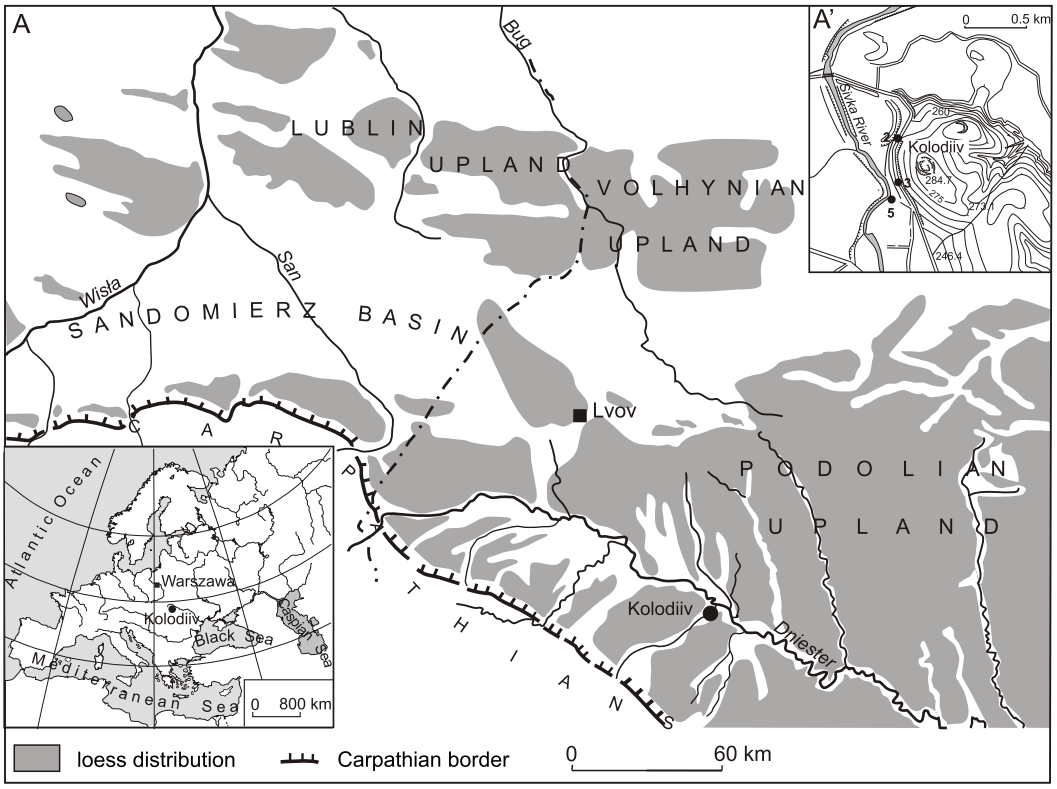

Fig. 1. A — location of profiles investigated at Kolodiiv; A' — sketch map of loess regional distribution (after Łanczont and Boguckyj, 2007)

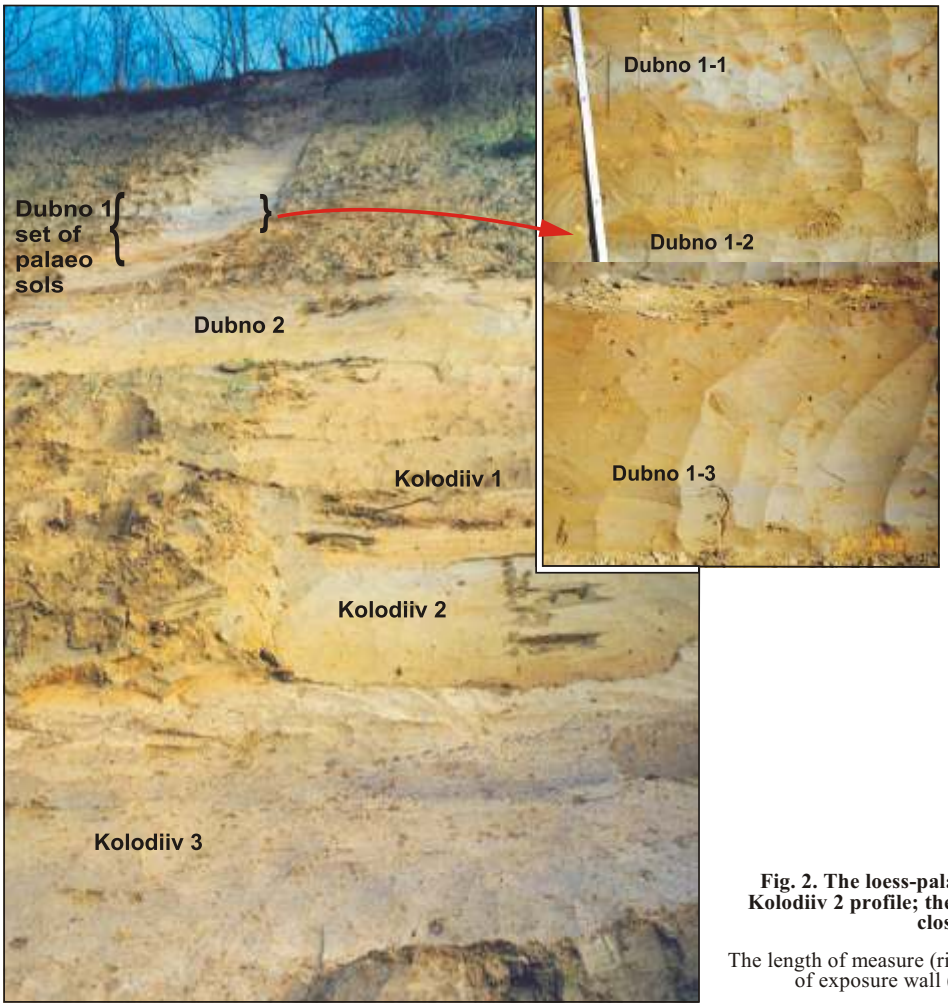

Fig. 2. The loess-palaeosol sequence of the Kolodiiv 2 profile; the Dubno 1 set of soils in close-up

The length of measure (right photo) is 1 m; the high of exposure wall (left photo) is 16 m

(2002). For the micromorphological analysis of the Early Vistulian fossil palaeosols (Kolodiiv 1, 2 and 3), eight monolithic samples were taken. The uppermost palaeosol (Kolodiiv 1) consists of partly redeposited, brown (10 YR5/3) silt (destroyed A horizon) and reddish brown (7.5 YR5/4) loamy silt (B horizon). Iron-manganese concretions are present at both horizons. Mole tunnels filled with material from the overlying soil are present in the lower part of the B horizon.

In the horizon A of the middle palaeosol (Kolodiiv 2), 20–30 cm thick, very characteristic traces of a large fire are present: clods of burned loam, yellowish red (5 YR4/8), and reddish brown (5 YR 4/4) and charcoal. The upper part of the horizon A has traces of redeposition in its structure and contains small pebbles. In the lowest part of the horizon, dark reddish brown: 5 YR3/4, 5 YR3/2, small zoogenic structures are to be found as well as mole tunnels. The B horizon of this soil, 50 cm thick, greyish and yellowish brown (10 YR5/2, 10 YR5/8), contains small pebbles, iron-manganese concretions and zoogenic structures. The lowest (Kolodiiv 3) soil is greyish brown (10 YR5/2), and grey with yellowish brown spots (10 YR7/1, 10 YR5/8). Traces of stratification are visible as well as zoogenic structures, iron-manganese concretions and charcoal. Beneath the set of three soils, Eemian peat is present in the Kolodiiv 5 profile (Kalinovych, 2002; Sytnyk *et al*., 2003).

MINERALOGICAL AND GEOCHEMICAL ANALYSIS

MATERIALS AND METHODS

Besides the stratigraphic subdivision of the Kolodiiv succession, the sequence analysed consisting of three loess beds and seven palaeosols was divided into eight units, which are characterized according to the granulometric features (Frankowski *et al*., 2007).

To provide information on the processes that could influence the chemical composition and the variation of the element distribution in the sequence analysed, 40 bulk sediment samples representing all units from the Kolodiiv 2 profile were selected for chemical analysis. Furthermore, 13 samples of Early Vistulian palaeosols from the Kolodiiv 5 profile were also analysed. The mineral composition of silt and clay fractions was determined for 12 samples representing as follows: Holocene soil (unit I); loess L1-l1 (unit II); Dubno set of three soils (unit III); 2 samples from Dubno 2 soil (unit V); Kolodiiv 1 soil (unit VII), two samples from the Kolodiiv 2 soil (unit VII) and two samples from interglacial soils: SS1-I and SS1-II (unit VIII).

The mineral composition of the 50–2 μm silt fraction was analysed using non-oriented powder samples by means of X-ray diffraction (XRD). Diffraction patterns were recorded in the range 1–120°2θ, on a *SIGMA 2070* diffractometer using a position-sensitive detector with CoKα radiation. *DIFFRACTIONEL* software v. 03/93 was used to process the data obtained. The identification of clay minerals was carried out for the untreated, and ethylene glycol-saturated oriented samples of clay fractions (< 2 μm). X-ray diffractometer traces were recorded in the range 2–70°2θ with CoKα radiation.

For chemical analysis the samples were ground in an agate mortar and dried at 105°C until a constant weight was achieved. Loss on ignition (L.O.I.) was measured weighing dried samples before and after calcination at 950°C. The powdered samples were digested using HF and aqua regia solution with boric acid in a Teflon bomb using a microwave furnace (*MLS 1200 mega* produced by Milestone). Major and trace element concentrations were determined by the atomic absorption spectrometry (AAS) method using a *PU 9100X* spectrometer produced by Philips. For analyses of Ti, Si, Al, Cr, Sr, V and Ba, potassium was added to the solution as ionization suppressant and the nitrous oxide-acetylene flame was used. The concentration of Fe, Mn, Mg, Ca, Co, Ni, Zn and Rb was measured using an air-acetylene flame. For determination of Ca and Mg, lanthanum was added to the solution as releasing agent and for Rb caesium was used as ionization suppressant. The measurements of Pb concentration were done using a deuterium lamp for background correction. The K and Na concentrations were measured in the emission mode from the solution with caesium.

The content of organic C was determined for the ground samples by means of the Tiurin's method (Dobrzański, 1971). The organic carbon was oxidised by boiling the mixture of a sample with 0.4N $K_2Cr_2O_7$ solution and Hg_2SO_4 as the catalytic agent for 5 min. The back titration of $K_2Cr_2O_7$ excess remaining in the solution with 0.2N $FeSO_4$ solution was utilised to determine the carbon content. Data were assessed for accuracy and precision using a control system including blank samples of the loess roasted at 900°C and duplicate samples. Three blank samples were analysed for every batch of 20 samples. The results were expressed as dried samples at 105°C. The content of humus was calculated according to the following equation (Dobrzański, 1971):

$$\text{weight \% of humus} = \text{weight \% of } C_{org} \times 1.724$$

where: 1.724 is a coefficient corresponding to the ratio of humus/organic C, assuming that humus contains 58 weight % of carbon.

MINERAL COMPOSITION OF SEDIMENTS

Detrital quartz grains predominate in all silt fractions analysed (Fig. 3). Albite and potassium feldspars are minor components of the primary, detrital mineral phases. However, in only one sample (Kolodiiv 2 palaeosol) potassium feldspars appear to dominate over albite. The absence of the reflections of Fe and Mn hydroxides as well as indistinct reflections of phyllosilicates in the diffractometer patterns of non-oriented samples are probably due to the poorly ordered structure and diminutive crystal sizes of these mineral phases. Calcite and minor dolomite are common in the loess (unit II), though only dolomite was detected in some soil samples (I and VIII units).

Precise determination of clay mineral phases as well as estimation of the content of expanding layers in illite and smectite structures are difficult owing to the presence of fine quartz and rare carbonate grains in the sediment fractions < 2 μm (Fig. 4). The main components of the clay fraction are smectite, kaolinite, and very fine crystalline illite or degraded muscovite. Broadened and asymmetric 001 reflections of illite and kaolinite indicate the poor ordering of the structure of these minerals. Moreover, the slight shift of the 001 reflection of illite

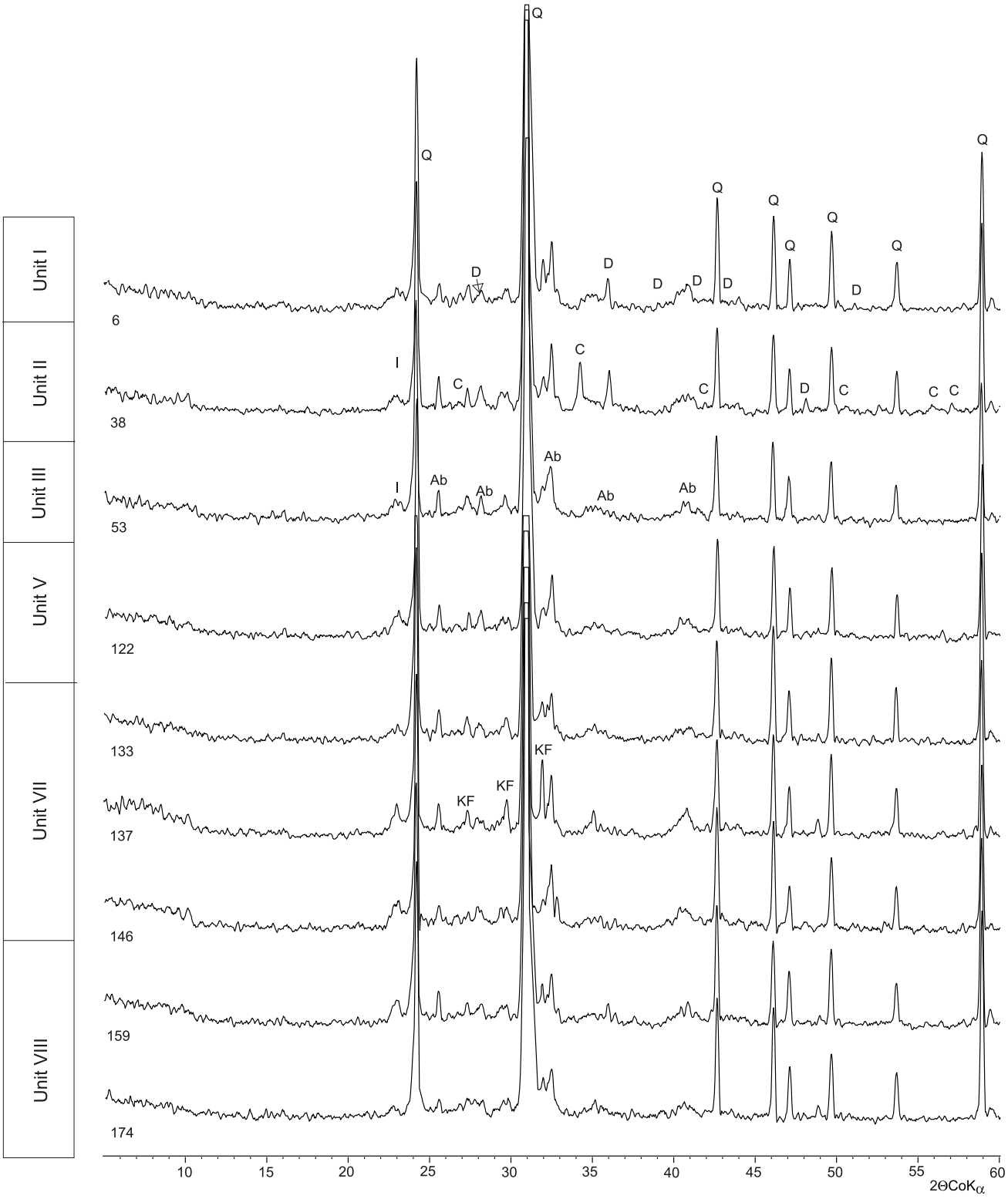

Fig. 3. XRD patterns of the non-oriented silt fraction from the Kolodiiv 2 profile

Q — quartz, C — calcite, D — dolomite, Ab — albite, KF — potassium-feldspar, I — illite, 6–174 — numbers of samples

and the appearance of a low angle tail in the X-ray tracing after ethylene glycol saturation of oriented samples (Holocene soil and underlying loess) may suggest the presence of an illite-smectite-like phase in the uppermost two units. The clay mineral composition of deposits along the profile analysed seems to be almost constant, although smectite and kaolinite are the main components of the clay fraction and illite is absent or occurs in traces in units III to VIII.

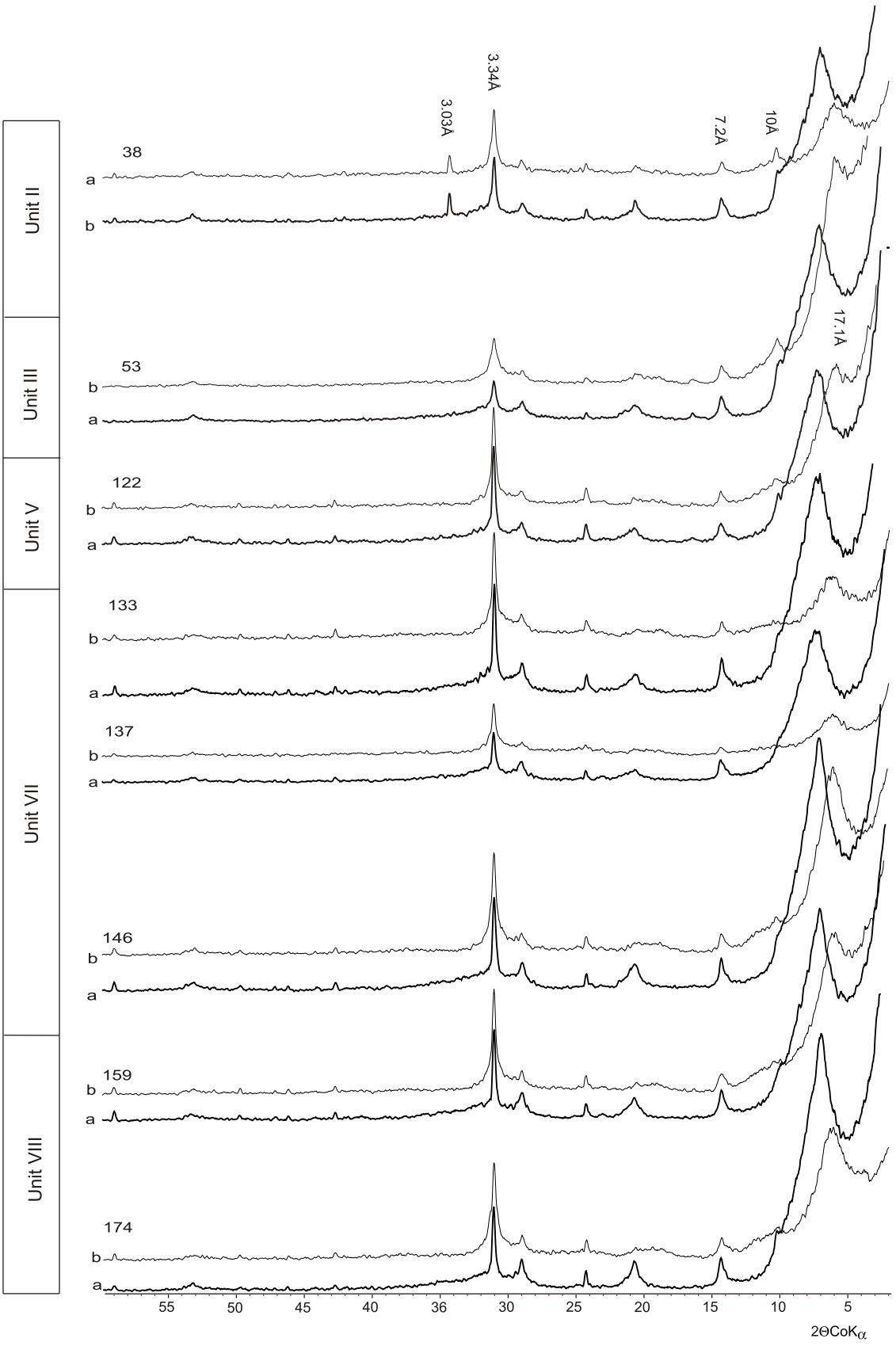

Fig. 4. XRD patterns of the raw and ethylene glycol-solvated clays from the < 2 μm size fraction from the Kolodiiv 2 profile

a — raw sample, **b** — ethylene glycol-solvated sample; other explanations as in Figure 3

All recognised mineral phases of clay fractions: kaolinite, smectite, illite, and illite-smectite could be either primary (detrital) or authigenic soil components. Each of these clay mineral phases may be a weathering product transported to the place of deposition or might originate due to the alteration of parent material and/or neoformation during pedogenesis (Curtis, 1990; Perederij, 2001). The intensity of weathering and soil-forming processes depends mainly on temperature and rainfall, which strongly influence the hydrolysis of detrital soil components. The association of smectite and kaolinite is common for soils, which were formed in humid climates with a long residence time of porewater (Curtis, 1990). The presence of illite in soils, particularly in the uppermost surface soil, may indicate a lower intensity of alteration processes within soil caused by lower precipitation and/or lower temperature (Curtis, 1990, 2003). Therefore, the mineral composition of clay fractions from the Dubno and Kolodiiv palaeosols probably reflects more humid palaeoenvironmental conditions during pedogenesis, than during the development of soils in the other parts of the profile analysed.

GEOCHEMISTRY OF THE DEPOSITS

The total concentrations of nine major (Si, Ti, Al, Fe, Mn, Mg, Ca, K and Na) and nine trace elements (Zn, Pb, Ni, Rb, Cr, Sr, Ba, Co, V) as well as the humus content and loss on ignition (L.O.I.) were measured. The results of chemical analysis are shown as the oxide (major elements) and element (trace elements) distribution profiles (Figs. 5, 6 and 7).

One of the most important factors that controls the chemical composition of the soils is soil parent material because many elements are fairly resistant to pedogenic processes. The index of alteration — CIA (chemical index of alteration) is used to evaluate the alteration processes that affect the composition of source material. The CIA is defined as CIA = $[Al_2O_3/(Al_2O_3 + CaO + Na_2O + K_2O)] \times 100$, in molar proportion, where CaO is the amount of CaO in silicates. Because the CO_2 content has not been measured, the CaO-silicates was calculated using the procedure of McLennan (1993), in which it is assumed that the number of CaO moles should not be greater than the number of Na_2O moles. The CIA values 50–55 indicate that loess particles (unit II) were derived from a poorly weathered source deposit. The slightly higher CIA values, 58–65, for sandy loess (unit IV) suggest that the source material have at least undergone one sedimentary cycle (McLennan, 1993; Gallet *et al*., 1998).

Depth profiles of SiO_2 and Al_2O_3 concentrations (Fig. 5) show the opposite trend with two exceptions, the palaeosol succession of unit III and the loess L1.12 (unit IV). The content of quartz in sediments is one of the most important factors influencing the element distribution because of its diluting effect on the minor and trace element concentrations. The estimation of relative quartz content was allowed on the basis of the mineral composition of the deposits, and of the Al_2O_3, K_2O and Na_2O concentrations. Therefore, the quartz content is the result of the subtraction of the amount of SiO_2 structurally bounded to feldspars and smectite from the total SiO_2 concentration. The vertical variation in quartz concentration shows an increase down the profile reaching a maximum value in units V to VII. Moreover, the quartz abundance clearly increases in the palaeosols developed on redeposited sediments in the upper part of unit III.

Despite clearly visible Al_2O_3 enrichment in units III and IV, the K_2O and Na_2O concentrations are nearly constant throughout the profile (Fig. 5). Thus, this might be an expression of the clay mineral composition as supported by XRD data, which show increasing contents of smectite and kaolinite in these units.

The vertical distribution of L.O.I. indirectly reflects the content of mineral phases that underwent thermal decomposition at 950°C (carbonates and clay minerals) as well as the content of organic carbon. Within units I and II, the variation of L.O.I. (Fig. 6) value parallels the variation of CaO and MgO (Fig. 5). Thus, the higher values of L.O.I. in these units are mainly due to the occurrence of carbonates. The same explanation seems to be valid for slight fluctuations of the L.O.I. values concomitant with CaO and MgO distribution in unit VIII, where dolomite was detected by XRD analysis. In the other parts of the profile the L.O.I. values generally reflect the distribution of organic carbon and clay minerals.

Distributions of Fe_2O_3 and MnO concentrations throughout the Kolodiiv 2 and Kolodiiv 5 profiles are nearly parallel, showing significant variation within the units from III to VIII (Figs. 5 and 7). An interesting exception to this pattern is unit III, where MnO accumulates in the horizon just above the maximum of total iron concentration. An inverse relationship between Fe_2O_3 and MnO concentrations is observed at the border of a palaeosol (unit V) with the underlying sandy loess (unit VI). Accumulation of hydroxides of Fe and Mn varies significantly according to redox conditions, which are related to the organic carbon degradation rate and to the abundance of fine silt and clay particles. As the result of the redox potential variations, manganese could be more quickly dissolved in reduced deposits than iron, and then Mn^{2+} may migrate to the oxic zones, where it reprecipitates as an oxyhydroxide of Mn^{4+} (Crerar, 1971/72; Hem, 1972; Yakimenko, 1995; Sterckeman *et al*., 2004; Wolthoorn *et al*., 2004).

The trace element concentrations range as follows: Cr from 36 to 85, V from 30 to 125, Co from 40 to 93, Ni from 40 to 116, Zn from 26 to 107, Pb from 26 to 63, Rb from 17 to 103, Sr from 26 to 119 and Ba from 66 to 495 ppm. The vertical distributions of Sr and Ba (Fig. 6) closely reflect those of CaO and MgO (Fig. 5), though Sr and Ba distribution profiles show significant horizontal variations throughout the unit III. Moreover, neither Rb distribution profile is similar to the vertical distribution of K, nor do Co, Ni, Zn, Pb, Cr and V distribution profiles parallel those of Fe_2O_3 and MnO (Figs. 5 and 6).

The relation between the loess and the Holocene soil in succession from the Kolodiiv 2 sequence (unit II and I, respectively) should provide information on the behaviour during pedogenesis of the elements analysed. To show the changes in element concentrations we have chosen the ratio of the element concentration in soil to that in loess (Table 1). The vertical distribution of these ratios shows soil enrichment in Fe_2O_3, MnO, Al_2O_3 and TiO_2 as well as Zn, Pb, Rb and V, and depletion in CaO, MgO and Sr with respect to loess. The concentrations of SiO_2, K_2O, Na_2O, Cr, Ni and Co show only insignificant vertical variations. The cycling of Fe, Mn is associated with the high mobility of these elements under anoxic conditions and their migration and reprecipitation in the oxic zone. The sharp in-

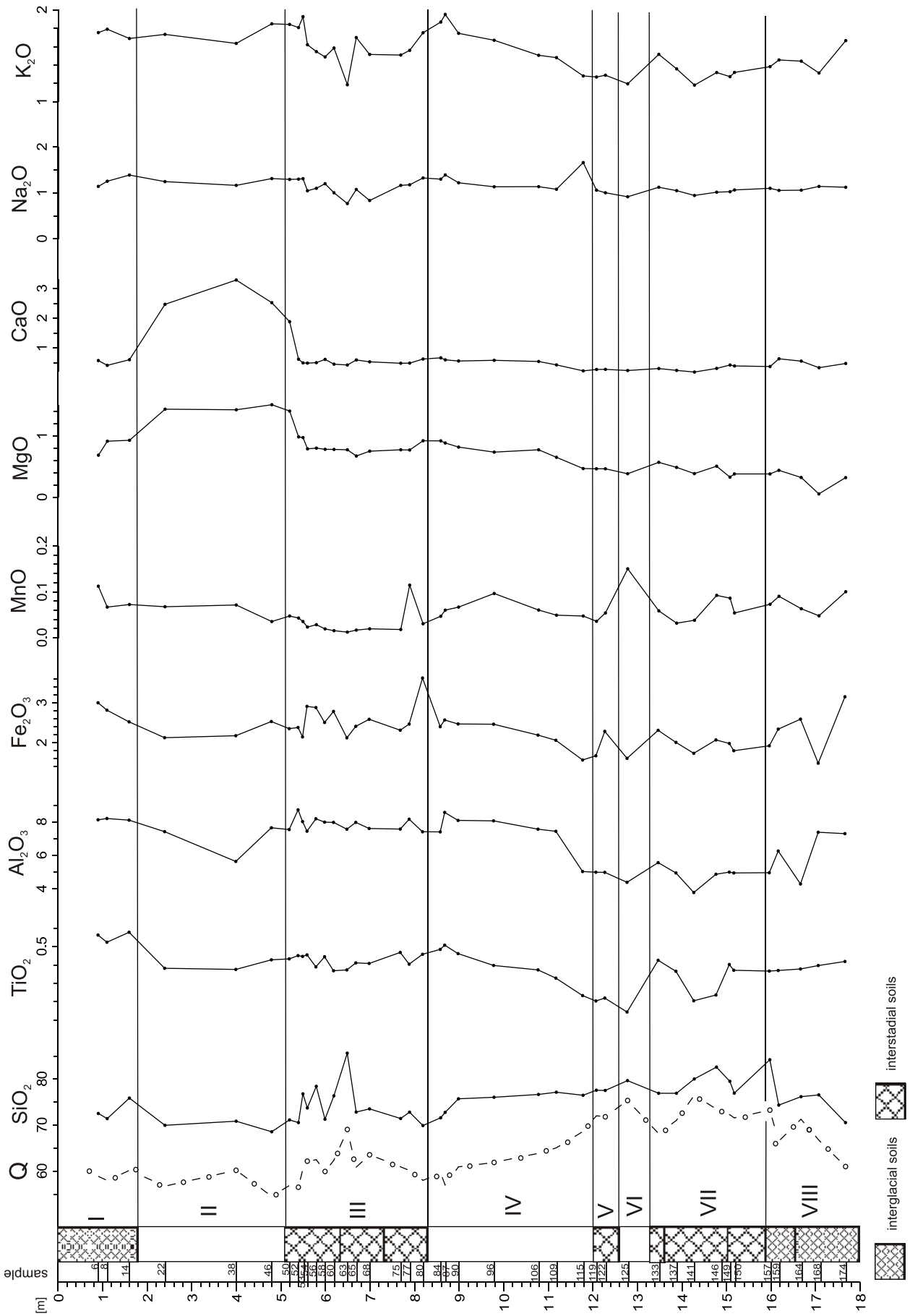

Fig. 5. Distribution of major elements contents (in weight %) in the Kolodiiv 2 profile

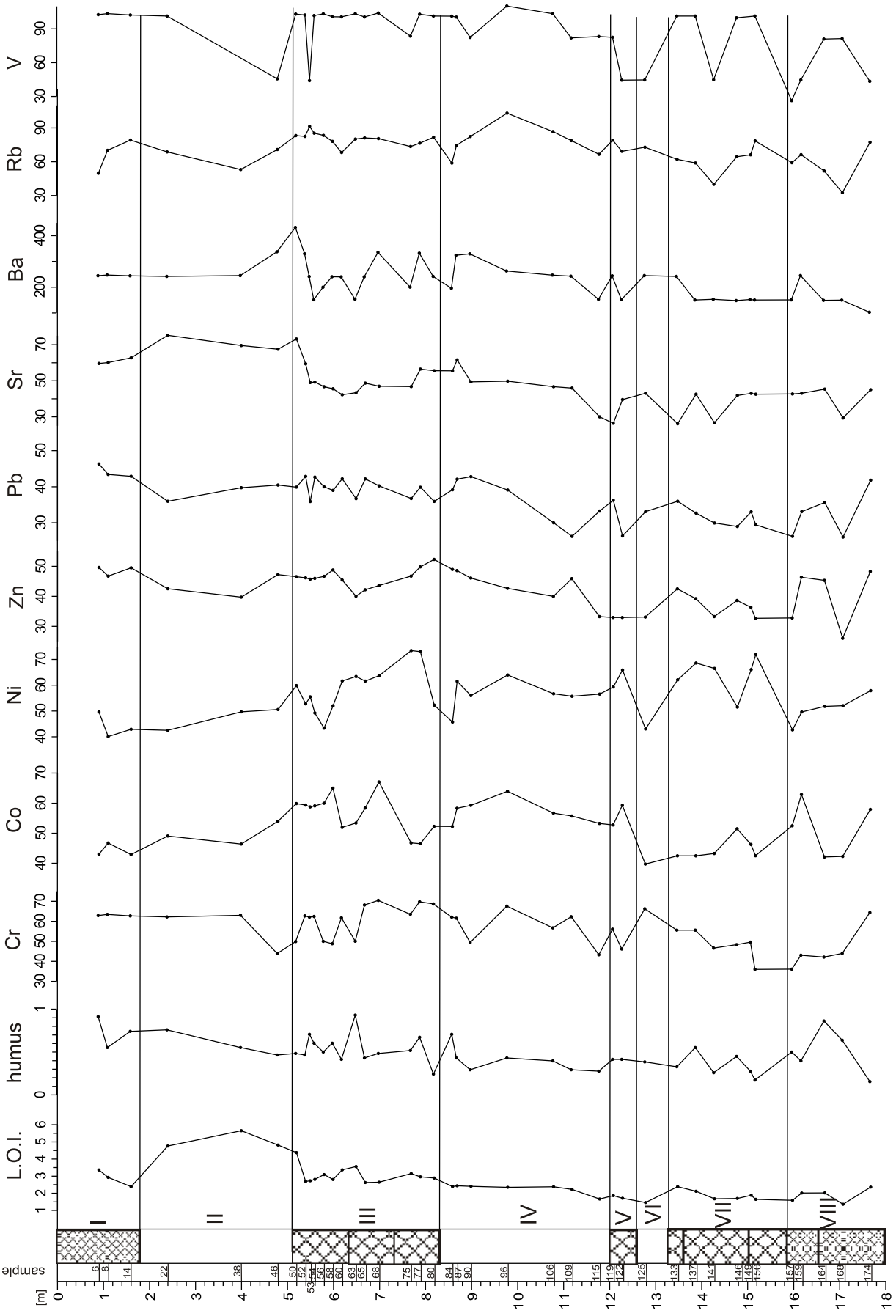

Fig. 6. The variation of L.O.I. and distribution of humus (in weight %), and trace element concentration (in ppm) in the Kolodiiv 2 profile

Explanations as in Figure 5

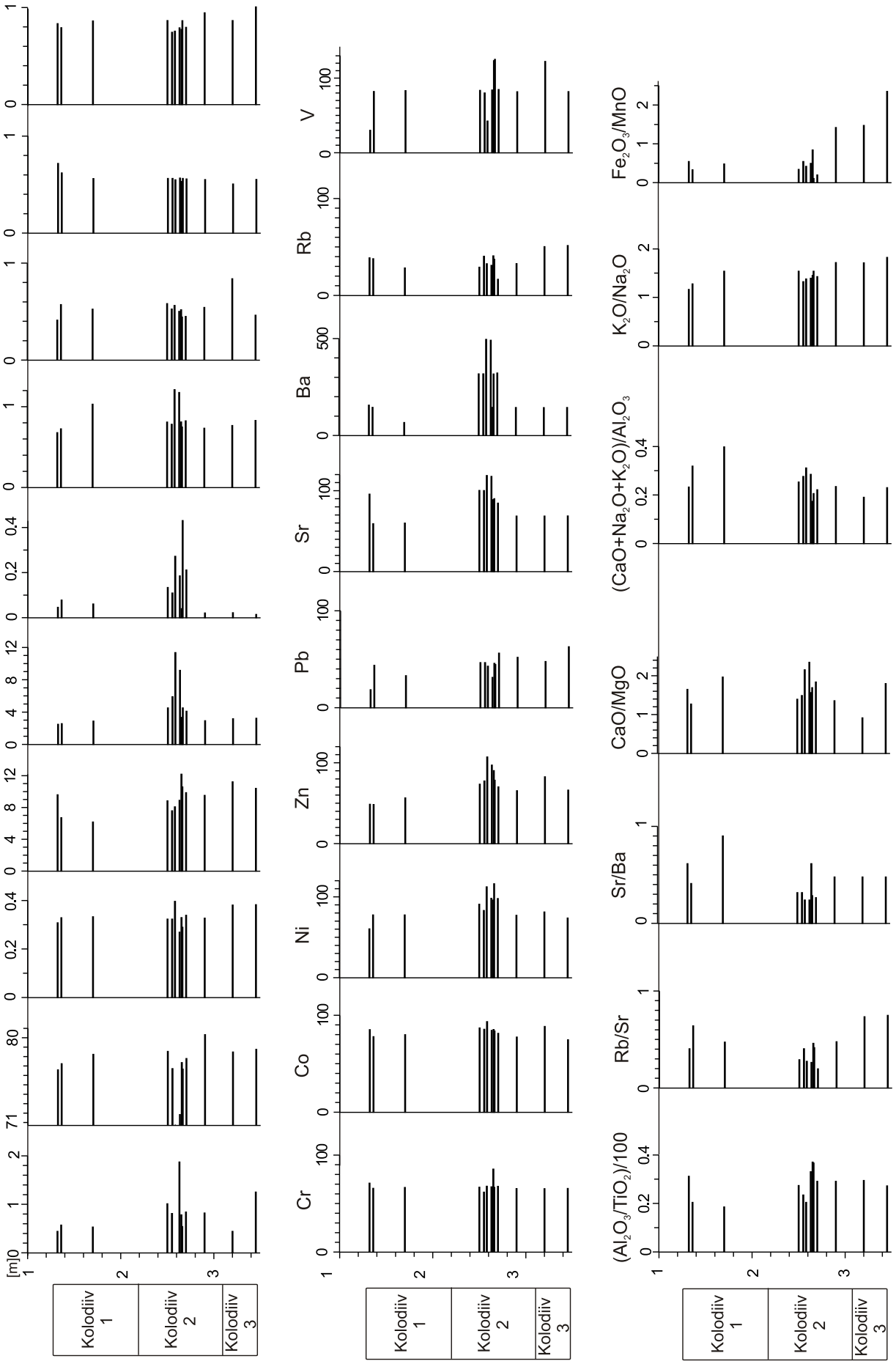

Fig. 7. Distribution of humus and major elements (in weight %) and trace elements (in ppm) and the variation in the concentration ratios of weathering-sensitive elements to relatively less mobile ones *versus* depth for the Kolodiiv 5 profile

Table 1

Variation of the loess-normalised major and trace element concentrations in Holocene soil

Sample no.	Holocene soil			Loess	
	6	8	14	22	38
Depth [m]	0.9	1.1	1.6	2.4	4.0
Ti/Ti_{loess}	1.47	1.36	1.51	0.99	1
Si/Si_{loess}	1.02	1.01	1.07	0.99	1
Al/Al_{loess}	1.44	1.46	1.44	1.32	1
Fe/Fe_{loess}	1.38	1.30	1.16	0.98	1
Mn/Mn_{loess}	1.45	0.86	0.93	0.87	1
Mg/Mg_{loess}	0.48	0.64	0.65	1.01	1
Ca/Ca_{loess}	0.17	0.12	0.18	0.75	1
K/K_{loess}	1.07	1.09	1.03	1.06	1
Na/Na_{loess}	0.99	1.08	1.20	1.07	1
Cr/Cr_{loess}	1	1.01	0.99	0.99	1
Co/Co_{loess}	0.93	1.02	0.93	1.07	1
Pb/Pb_{loess}	1.16	1.08	1.07	0.90	1
Ni/Ni_{loess}	0.99	0.80	0.86	0.85	1
Zn/Zn_{loess}	1.24	1.17	1.24	1.06	1
Sr/Sr_{loess}	0.85	0.86	0.90	1.07	1
V/V_{loess}	3.42	3.45	3.41	3.38	1
Ba/Ba_{loess}	1	1.01	1	0.99	1
Rb/Rb_{loess}	0.94	1.32	1.49	1.30	1

crease in Mn and V accumulation in the uppermost horizon of unit I, and the moderate increase in Pb and Zn, probably result from biochemical cycling of elements and/or have an anthropogenic source. The biochemical mechanism of micronutrient uptake, such as Mn and Zn, by roots results in their accumulation with plant residue (Kabata-Pendias and Pendias, 1999; Sterckeman *et al*., 2004).

RESULTS OF DATA PROCESSING

In order to reveal factors affecting the element distributions in the Kolodiiv 2 and 5 profiles, the correlations between elements, humus content and also clay, silt and sand mineral fractions were calculated (Table 2) and the factor analysis was performed using the *STATISTICA* software (1993). Most of the elements studied did not show any distinct correlation with the content of the sand, silt or clay fraction. The insignificant correlation between the clay mineral content and trace elements may suggest that clay minerals are only one of the factors influencing the distribution of trace elements in these deposits. The correlation coefficients between humus content and Fe_2O_3, Zn, Sr, Al_2O_3, Co, Pb, Ni, MnO and Ba concentrations are moderately positive and range from 0.33 (Pb) to 0.66 (Zn) and 0.71 (Fe_2O_3). The above mentioned trace elements and additionally Cr are positively correlated with Al_2O_3 and Fe_2O_3. Moreover, Ni, Zn and Ba are moderately linked to MnO. Positive correlation of trace elements with aluminium and iron might imply that aluminosilicates, hydroxides of Fe and, to lesser degree, Mn hydroxides are their carrying phases. The correlation coefficients between CaO, MgO, Sr and Ba range from 0.3 to 0.5. The values of the correlation coefficients between Sr and Al_2O_3, Fe_2O_3 and humus (0.63, 0.73 and 0.64, respectively), are slightly higher than this value for Sr and CaO (0.51). Thus, it is evident that in the deposits analysed strontium is not only structurally bound to carbonates but also seems to be adsorbed on to aluminosilicates, Fe hydroxides and humus. Rubidium strongly positively correlates with K_2O and Na_2O and moderately with the clay fraction, which may be due to the high affinity of Rb for clay minerals. The positive correlations between TiO_2, Cr, Al_2O_3, V and the silt fraction, and also the positive correlation between V and MgO can be attributed to the partitioning of these elements into detrital mica.

R-mode factor analysis (Davis, 1973) was applied to determine the main factors affecting the distribution of elements throughout the profile. Seven out of 22 factors reflect 83.1% of the total variance indicating the absence of direct correlation between most of the components in the set of 22 variables (Fig. 8). This would be expected because trace elements are generally associated with more than one carrying species or phase. However, they are essentially associated with the fine, frequently colloidal, organic and mineral adsorbing phases (Öhlander *et al*., 2003; Sterckeman *et al*., 2004). Therefore, the element distribution may be influenced by a number of independent factors causing simultaneous enrichment with these elements. The first factor (30.6% of total variability) reflects the variation in the Co, Ni, Zn, Sr, Fe_2O_3, and Al_2O_3 contents against the variation in Na_2O, K_2O and Rb concentrations. Therefore, Co, Ni, Zn and Sr seem to be mainly associated with Fe hydroxides and clay minerals such as kaolinite and smectite. Nevertheless, the vertical variation of Fe_2O_3, MnO and Ba (factor 4 responsible for 7% of total variability) emphasizes horizons enriched with manganese (Fig. 5). Oxidation-reduction processes also have a noticeable effect on the distribution of Mn and Ba. Higher Mn may be the result of the higher solubility of this element under acid and slightly reducing conditions, and its precipitation when conditions become basic and/or aerobic (Crerar *et al*., 1971/72; Hem, 1972). Such changes are observed within soil profiles where manganese is distributed from the A to B soil horizon (Sterckeman *et al*., 2004). The enrichment of Fe and Mn hydroxides with Ba results from the scavenging of dissolved Ba species, which was released to porewaters mainly by the degradation of the Ba-containing minerals. Variation in the V and Pb association (factor 6, 4.9% of total variability) is noticeably parallel to the variation in factor 7 (the humus content) only in the Holocene soil. In other soil units of the Kolodiiv 2 sequence the interdependence of V, Pb and humus accumulations is less obvious (Fig. 6). Factor 2 (20.4% of total variability) represents the variation of carbonate content (the association of CaO, MgO, Sr and Ba) that is inverse to the SiO_2 variation. Factor 3 (11.3% of total variability) reflects granulometric variation in the deposits, i.e. the variation in sand and silt abundance. Two of the seven factors reflect variation of components which are not directly associated with the others: factor 5 (5.1% of the total variability) shows the distribution pattern of the clay content in the sequence, and factor 7 (3.8% of the total variability) the distribution of humus.

Table 2

Correlation coefficients for humus, major and trace element concentrations, and granulometric characteristics of the deposits from the Kolodiiv 2 and Kolodiiv 5 profiles

	Clay	Silt	Sand	Humus	TiO_2	SiO_2	Al_2O_3	Fe_2O_3	MnO	MgO	CaO	Na_2O	K_2O	Cr	Co	Pb	Ni	Zn	Sr	V	Ba	Rb
Clay	1																					
Silt	–0.12	1																				
Sand	–0.44	–0.84	1																			
Humus	–0.16	0.13	–0.02	1																		
TiO_2	0.13	0.31	–0.35	0.04	1																	
SiO_2	–0.11	–0.02	0.08	0.01	–0.50	1																
Al_2O_3	–0.05	0.37	–0.31	0.41	0.43	–0.24	1															
Fe_2O_3	–0.16	0.24	–0.13	0.71	0.00	–0.21	0.45	1														
MnO	–0.31	0.17	0.01	0.32	–0.20	0.01	–0.01	0.47	1													
MgO	0.06	–0.07	0.03	0.01	0.45	–0.56	0.29	–0.02	–0.22	1												
CaO	–0.21	–0.23	0.32	0.21	0.13	–0.47	0.16	0.16	0.06	0.72	1											
Na_2O	0.22	–0.22	0.08	–0.45	0.40	–0.47	–0.31	–0.45	–0.21	0.39	0.04	1										
K_2O	0.22	0.01	–0.13	–0.34	0.64	–0.58	–0.07	–0.34	–0.27	0.59	0.16	0.84	1									
Cr	–0.16	0.35	–0.23	0.27	0.16	–0.29	0.59	0.38	0.18	0.20	0.10	–0.31	–0.07	1								
Co	–0.18	0.25	–0.13	0.37	–0.16	0.09	0.65	0.56	0.13	–0.05	0.12	–0.67	–0.57	0.41	1							
Pb	–0.05	0.18	–0.14	0.33	0.38	–0.17	0.59	0.24	0.02	0.27	0.18	–0.21	0.05	0.40	0.29	1						
Ni	–0.17	0.17	–0.06	0.40	–0.28	0.19	0.32	0.56	0.30	–0.29	–0.05	–0.69	–0.68	0.30	0.61	0.25	1					
Zn	–0.21	0.31	–0.17	0.66	0.09	–0.13	0.70	0.85	0.32	0.09	0.20	–0.59	–0.42	0.52	0.75	0.50	0.64	1				
Sr	–0.33	0.17	0.03	0.64	0.10	–0.26	0.63	0.73	0.42	0.29	0.51	–0.43	–0.30	0.51	0.66	0.29	0.44	0.79	1			
V	0.08	–0.02	–0.03	0.10	0.41	–0.20	0.25	0.08	–0.14	0.33	0.07	0.10	0.21	0.24	–0.09	0.37	0.07	0.15	0.03	1		
Ba	0.00	0.11	–0.10	0.31	0.18	–0.48	0.33	0.48	0.38	0.47	0.34	0.14	0.26	0.25	0.15	0.19	0.16	0.35	0.47	0.19	1	
Rb	0.38	–0.02	–0.19	–0.45	0.30	–0.23	–0.11	–0.38	–0.36	0.39	–0.12	0.63	0.71	–0.08	–0.40	–0.08	–0.51	–0.45	–0.44	0.22	0.15	1

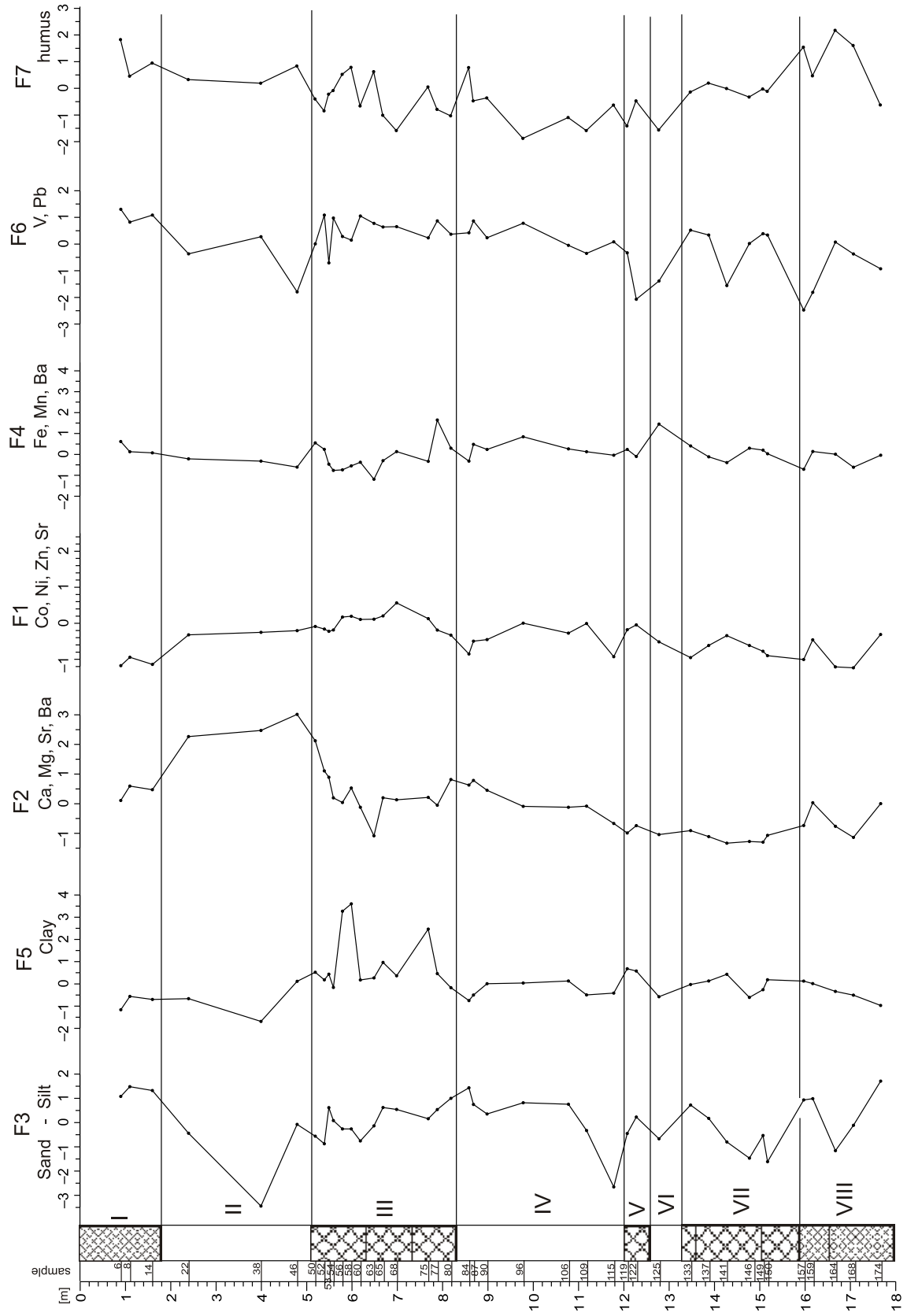

Fig. 8. Distribution of factor scores from the R-mode factor (F) analysis of the samples from the Kolodiiv 2 profile on the basis of the granulometric and chemical compositions

Explanations as in Figure 5

THE GEOCHEMICAL INDICES OF THE CLIMATIC CHANGES

Climatic conditions strongly influence the mobilization and accumulation of elements in soil profiles due to changes in the intensity of weathering and pedogenic processes. The intensity of these processes depends on precipitation, temperature, chemical composition of soil water, and also on the development of vegetation (Curtis, 1990, 2003; Catt, 1991). Geochemical indices of the intensity of pedogenic processes are based on the variation of the concentration ratio of weathering-sensitive elements to persistent ones (e.g. aluminium and titanium expressed as Al_2O_3/TiO_2 ratio; Zhang and Frost, 2002). Moreover, the intensity of pedogenesis may be illustrated by the variation of concentration ratio of the relatively more to relatively less mobile elements (e.g. Rb/Sr and Sr/Ba) (Dasch, 1969; Gallet *et al*., 1998; Zhang and Frost, 2002). Lower values of these ratios reflect strong weathering and/or high mobility of a given element in the soil arising usually from warmer and wetter climatic conditions. In this way, the slight decrease in the values of Rb/Sr ratio for the SS1- (I + II), Kolodiiv 3, and Kolodiiv 2 palaeosol units may indicate warming and/or higher precipitation (Figs. 7 and 9). Moreover, the distinct increase in these values from the upper part of unit VII to unit III may indicate cooler and/or a less humid climate under which the Kolodiiv 1, Dubno 2 and Dubno 1 soil succession were developed. The fluctuation in the values of Al_2O_3/TiO_2 ratio is not as great as that in the Rb/Sr ratio. Nevertheless, the Al_2O_3/TiO_2 ratio also increases in the units from VI to III. The vertical variation in the values of the Sr/Ba ratio shows sharp fluctuations in all soil units, above all in the Dubno 1 soil. The changes in this value result mainly from the variation in the Ba concentration, because the Sr concentration is almost constant throughout the Dubno 1 soil. The similarity of the Sr/Ba and Fe_2O_3/MnO variations are probably the result of barium cycling, which arises from changes in the redox conditions during pedogenesis.

To show the intensity of weathering and pedogenesis in loess-palaeosol sequences that reflect palaeoclimatic conditions Hum (1997) applied the variation of in CaO/MgO, $(CaO+K_2O+Na_2O)/Al_2O_3$ and K_2O/Na_2O ratios. Warmer and wetter climates cause an increase in carbonate dissolution and Al_2O_3 concentration and also promote clay mineral formation. Thus, during warm humid intervals the CaO/MgO and $(CaO+K_2O+Na_2O)/Al_2O_3$ ratios decrease and the K_2O/Na_2O ratio increases (Hum, 1997). In soil units of the Kolodiiv 2 sequence the variation in CaO/MgO is nearly constant. In the Dubno 1 soil the values of the $(CaO+K_2O+Na_2O)/Al_2O_3$ ratio decrease and the values the K_2O/Na_2O ratio increase, indicating a rise in humidity and/or temperature during the formation of this well-developed soil.

MICROMORPHOLOGY OF THE VISTULIAN INTERSTADIAL SOILS

For the micromorphological study, samples from the Kolodiiv 5 and 3 profiles were used. The profiles descriptions are in Łanczont and Boguckyj (2002). Eight thin sections from the Kolodiiv 5 profile and four from the Kolodiiv 3 profile represent individual palaeosols distinguished during field logging and designated as Kolodiiv 1 (the youngest), 2 and 3. According to the description made during field analysis of the Kolodiiv 5 profile, two samples were taken from the Kolodiiv 1 soil, four from the Kolodiiv 2 soil, and two from the Kolodiiv 3 soil. An additional four thin sections were made from the Kolodiiv 1 and 2 soils of the Kolodiiv 3 profile. Five thin sections represent the Dubno set of palaeosols, two from the Kolodiiv 5 profile, and three from the Kolodiiv 3 profile.

In the analysis, special attention was given to the presence and intensity of traces of pedological processes, namely: different colloidal clays; the types and distribution of organic matter; the forms, mineral composition and distribution of concretions; the presence and shapes of biopores.

KOLODIIV SET OF PALAEOSOLS

The micromorphology does not exactly reflect the division of the Kolodiiv set of soils into three separate soils observable at exposure. Three thin sections from the lowest part of the set in the Kolodiiv 5 profile show similar compositions. Some rocks fragments (mudstones mainly) are present in the soil matrix. A slightly separated clay — plasma (in palaeopedological nomenclature) of lattisepic type is present as small concentrations, and plasma of skelsepic type (Fig. 10A) was observed sporadically around bigger quartz grains. Various ferruginous precipitations are present (Fig. 10B, C and D). Chemical analysis confirms that they are iron rather than, manganese-iron precipitations. Some organic matter is present here, mainly filling voids. Probably it was translocated by percolating water from organic-rich overlying layers. Locally, there are empty rounded or elongated pores. Significant bioturbation traces are present.

Three thin sections from the middle part of the set (described in the field as the Kolodiiv 2 palaeosol) represent a chernozem soil, rich in humus. An admixture of grains coarser than loess, of quartz and feldspars, is present. The thin section of the uppermost sample of the set, represents the upper part of the A horizon of a soil with slightly separated plasma, without any orientation in its distribution. Organic matter is present as mullicol and mulliskel, locally with fragments of plant tissue, and burned wood or other plant fragments. In places, organic matter forms agglomerates with iron oxide precipitations (Fig. 10E) and, dispersed small iron-humus concretions. Some pores are coated with organic matter. In the thin section representing the middle part of the A horizon of the soil, numerous burned pieces of wood are present, evidence of a large fire in the vegetation cover. Concentrations of organic matter and small ferruginous (goethite) concretions with a substantial iron content are visible in the section, and were confirmed by chemical analysis. The thin section of the lowest part of the chernozem A horizon shows a low content of organic matter and empty pores of biological origin. Weak traces of the fire are present, probably on a secondary bed.

Thin sections from the uppermost part of the Kolodiiv set of soils (Kolodiiv 1 soil) represent a weakly developed gley soil. The parent material contains sand grains of quartz and feldspars. The soil plasma is very slightly segregated (Fig. 10F), without regular orientation. Pores exist as straight

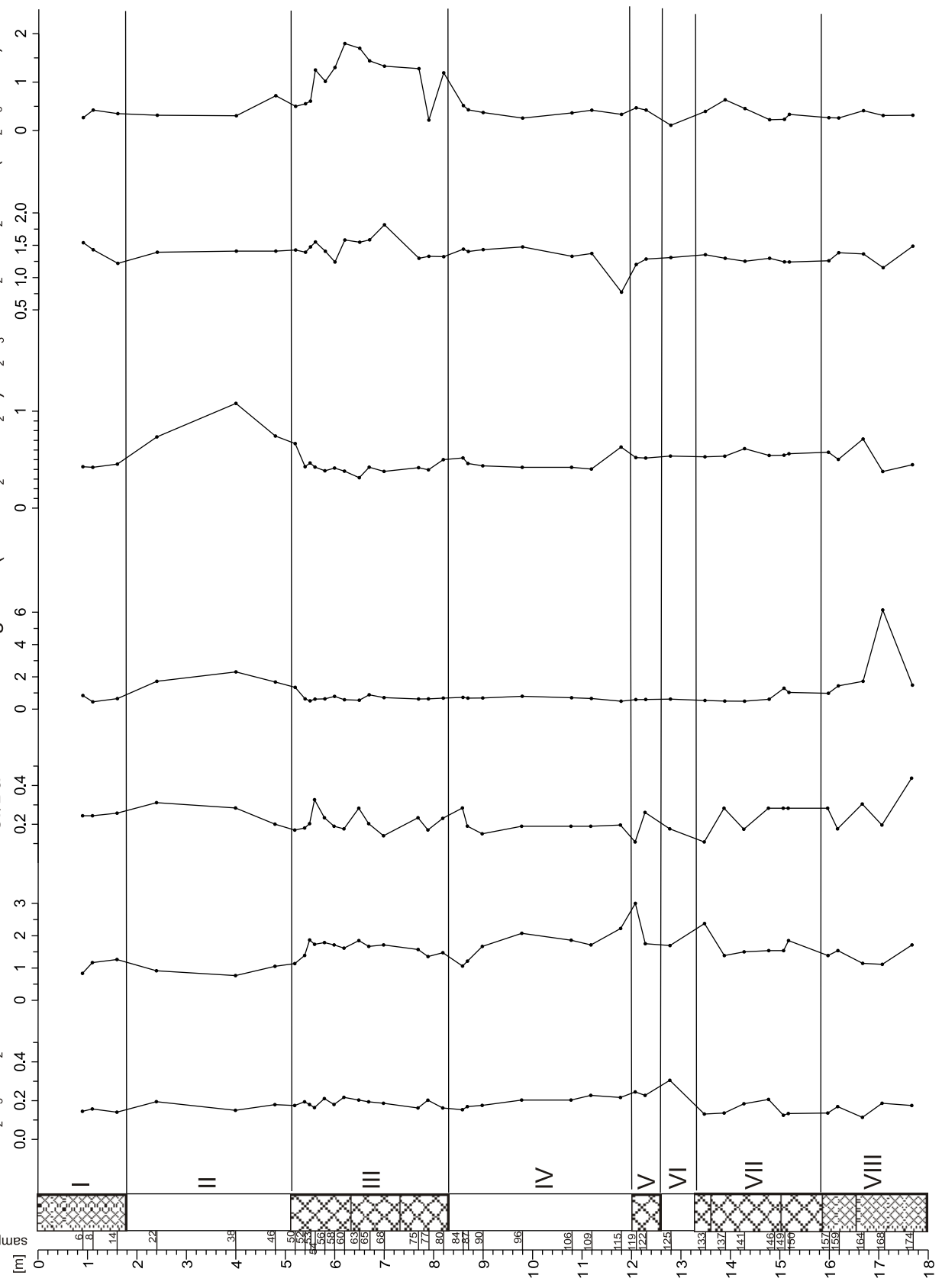

Fig. 9. The variation in the concentration ratios of weathering-sensitive elements to relatively less mobile ones for the Kolodiiv 2 profile

Explanations as in Figure 5

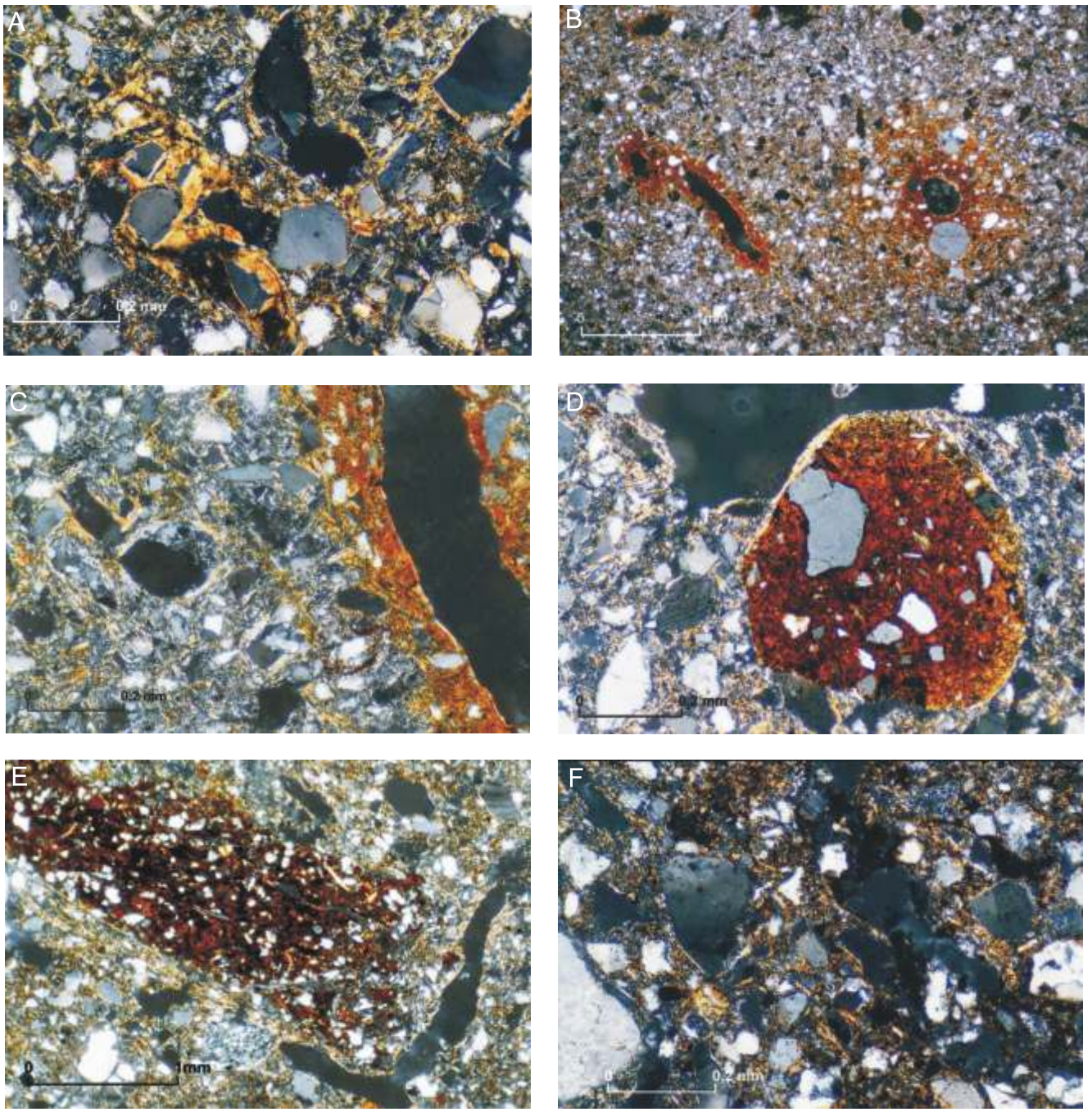

Fig. 10. Micromorphology of the Kolodiiv palaeosols

A–**C** — Kolodiiv 3 palaeosol (crossed polars): A — clay particles coat the quartz grains, B — ferrugineous precipitations are present around the pores, C — clay minerals are dispersed and randomly oriented in the soil matrix and ferrugineous precipitations are present around the pores; **D**, **E** — Kolodiiv 2 palaeosol (crossed polars): D — ferrugineous, clay papula, E — organic matter and iron oxide precipitation and an elongated empty channel; **F** — Kolodiiv 1 palaeosol (crossed polars) clay minerals weakly segregated around quartz grains and small papules of iron oxides and organic matter

or curved, usually empty, channels. A small amount of organic matter is present. Small concretions composed of iron compounds and organic matter are present as well as redeposited fragments of ferruginous concretions, some of these with admixed organic matter.

According to K. Konecka-Betley (pers. comm.), the set of Kolodiiv 1–3 soils of the Kolodiiv 5 profile represent two Early Vistulian, interstadial-type palaeosols only. The older soil, calcic chernozem in type, corresponds with both Amersfoort and Brörup interstadials. A thick horizon of mollic-type humus indicates intensive development of pedogenic processes leading to chernozem formation. No traces of luvisol were found. The sediments distinguished in the field as the Kolodiiv 3 soil, according to K. Konecka-Betley, represent the C horizon of

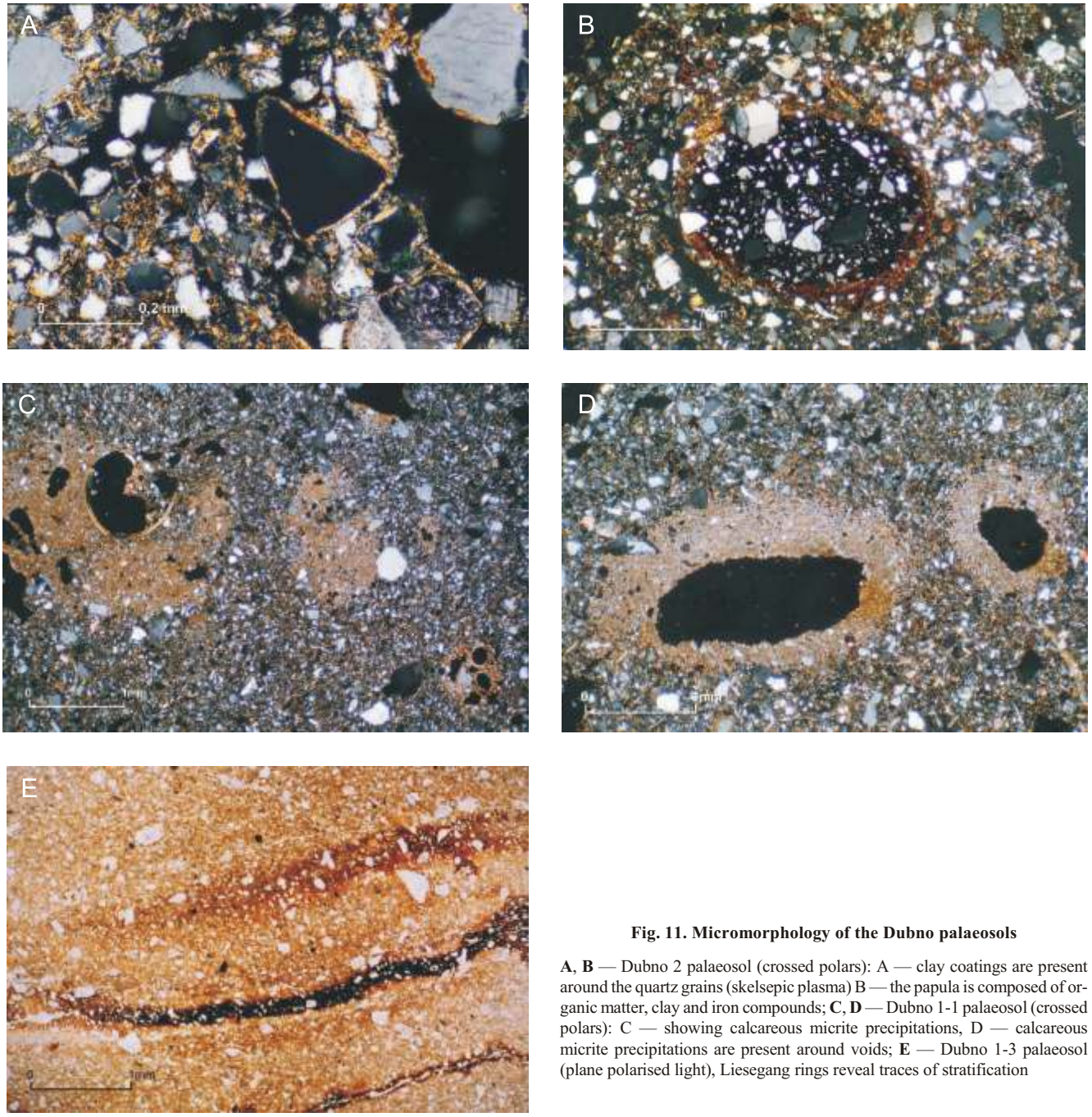

Fig. 11. Micromorphology of the Dubno palaeosols

A, **B** — Dubno 2 palaeosol (crossed polars): A — clay coatings are present around the quartz grains (skelsepic plasma) B — the papula is composed of organic matter, clay and iron compounds; **C**, **D** — Dubno 1-1 palaeosol (crossed polars): C — showing calcareous micrite precipitations, D — calcareous micrite precipitations are present around voids; **E** — Dubno 1-3 palaeosol (plane polarised light), Liesegang rings reveal traces of stratification

a chernozem soil, though redeposited organic material (humus) occur there. Thin sections from the uppermost part of the set document the younger soil, an eutric gleysol, corresponding to the Odderade Interstadial.

The micromorphological picture of thin sections of the Kolodiiv 3 profile differs from those described above. The soil matrix contains rounded and weathered fragments of mudstones and shales containing sand-sized iron compound as well as grains of quartz and feldspar. Elongated curved pores of the upper part are usually empty or contain an amorphous organic substance; in places fine silt material fills larger voids. Clay minerals are dispersed or concentrated around the matrix grains. Some calcite concretions are present. In the lower part of the Kolodiiv 3 profile the remnants of the B horizon of the Luvisol are visible in thin section; as clay minerals coating the voids (vosepic plasma: Fig.10A; as well as lattisepic and skelsepic). Probably this is part of a redeposited interglacial soil.

DUBNO SET OF PALAEOSOLS

Two thin sections were made from the Dubno 2 palaeosol from the Kolodiiv 5 profile. In the soil matrix, quartz and feldspar grains dominate, and are coarser in the upper part. Admixed fragments of mudstones are present. Clay minerals are rare in the upper part, and in the lower part are present in lattisepic, partly reticulate form. Clay coatings around the quartz grains are also present in places (skelsepic plasma; Fig. 11A). Organic matter, mullicol in form, is present in the upper part of the soil and is almost absent in its lower part. Sim-

ilarly, small concretions, composed of iron compounds and organic matter (Fig. 11B), are numerous in the upper part and scarce in the lower part. Voids and pores are small, rare, and usually empty. K. Konecka-Betley defined this horizon as initial Bbr, and the soil as a brown arctic one.

The micromorphological picture of the Dubno 1 set of palaeosols in the Kolodiiv 3 profile is similar to the lower part of the soil from the Kolodiiv 5 profile described above. Additionally some voids are present, filled or coated by precipitations of ferruginous and manganese compounds. Calcite precipitations are common in the uppermost soil (Fig. 11C and D).

Beside the palaeopedological characteristics, some important features are visible in thin sections, showing the redeposition of sediments and soils. The presence of coarse material (sand grains and stone fragments), besides the loess fraction, shows that aeolian processes were not the only depositional agent. The second feature is the existence of orientated (directional) structures inside the soils bodies (Fig. 11E). They support the field observations and document the strong influence of slope processes during sedimentation and pedogenesis.

CONCLUSIONS

1. The major element values of loess and sandy loess from the Kolodiiv 2 loess-palaeosol sequence indicate that the loess particles were derived from poorly weathered source rocks that have at least undergone one sedimentary cycle. The same conclusion was drawn from heavy mineral analysis (Racinowski, 2002).

2. Weathering and pedogenic processes have influenced the distribution of major and trace elements throughout the sequence. The correlation and factor analysis of humus, major and trace elements concentrations together with granulometric characteristics did not enable precise determination of the trace element-carrying phases. Insignificant correlation between the clay mineral content and all of the trace elements analysed suggests that clay minerals are not the main factor influencing the distribution of trace elements in these deposits. Zn, Co, Pb, Ni, Fe_2O_3, Al_2O_3, MnO, and in part Sr and Ba, are associated with humus. Despite the affinity of V and Pb for organic matter, the association of these elements with humus is clearly less close. Besides the humus, the second carrying phases for Sr seem to be carbonates. The association of Ba with hydroxides of manganese and iron points to the sensitivity of this element to redox conditions.

3. The intensity of weathering and pedogenic processes has been strongly influenced by climatic conditions because it largely reflects precipitation and the development of vegetation. Geochemical indices of the intensity of weathering and pedogenic processes, such as the Al_2O_3/TiO_2, Rb/Sr, and Sr/Ba ratios, indicate a warm and humid climate during the formation of the SS1, Kolodiiv 3 and 2 soil units. The increase in the values of these geochemical indices for the Kolodiiv 1, Dubno 2 and 1 soil units may indicate cooling and/or a reduction in precipitation. Nevertheless, the thickness of the very well-developed Dubno 1 soil, and the association of smectite and kaolinite in the clay size fraction, as well as distinct enrichment in Fe_2O_3, Al_2O_3, and variation in trace element concentrations in individual horizons indicate high precipitation.

4. The micromorphological analysis showed that the interstadial palaeosols examined represent Early Vistulian chernozem or gley type soils. However, genetic interpretation is difficult because these soils developed as redeposited sediments and/or they were partially denuded. The results obtained show a mosaic pattern and a spatial variability of these interstadial soil types in mesoscale, as deduced from geological-palaeogeographical studies (Łanczont and Boguckyj, 2002).

5. The soils of the Dubno 1+2 set examined represent a subarctic brown type. Redeposition of mineral and soil material is clearly visible in micromorphological sections.

6. The geochemical and palaeopedological analyses provided important evidence of the strong influence of redeposition processes (solifluction, slopewash) on the formation of the aeolian loess cover on the Pleistocene terraces of the Sivka River, as is directly reflected in the results of palaeomagnetic (Nawrocki *et al.*, 2007) and thermoluminescence (Kusiak, 2007) analyses.

REFERENCES

CATT J. A. (1991) — Soils as indicators of Quaternary climatic change in mid-latitude regions. Geoderma, **51**: 167–187.

CRERAR D. A., CORMICK R. K. and BARENS H. L. (1971/1972) — Organic control on the organic geochemistry of manganese. Acta Miner.-Petrograph., **20**: 217–226. Szeged.

CURTIS C. D. (1990) — Aspects of climatic influence on clay mineralogy and geochemistry of soils, palaeosols and clastic sedimentary rocks. J. Geol. Soc., London, **147**: 351–357.

CURTIS C. D. (2003) — The aqueous geochemistry of metals in the weathering environment: strengths and weaknesses in our understanding of speciation and process. Miner. Mag., **67**: 235–246.

DASCH E. J. (1969) — Strontium isotopes in weathering profiles, deep-sea sediments, and sedimentary rocks. Geochim. Cosmochim. Acta, **33**: 1521–1552.

DAVIS J. C. (1973) — Analysis of multivariate data. In: Statistics and Data Analysis in Geology: 468–620. John Wiley and Sons. New York.

DOBRZAŃSKI B. (1971) — Gleboznawstwo laboratoryjne: Oznaczanie próchnicy. In: Gleboznawstwo. Zajęcia praktyczne: 130–138. PWN, wyd. II. Warszawa.

FRANKOWSKI Z., ŁANCZONT M. and BOGUCKYJ A. (2007) — Vistulian litho- and pedosedimentary cycles recorded in the Kolodiiv loess-palaeosol sequence (East Carpathian Foreland, Ukraine) determined by laser grain-size analysis. Geol. Quart., **51** (2) : 147–160.

GALLET S., BOR-MING J., VAN VLIET LANOË B., DIA A. and ROSSELLO E. (1998) — Loess geochemistry and its implication for particle origin and composition of the upper continental crust. Earth Planetary Sci. Lett., **156**: 157–172.

HEM J. D. (1972) — Chemical factors that influence the availability of iron and manganese in aqueous systems. Geol. Soc. Am. Bull., **83**: 443–450.

HUM L. (1997) — Palaeoenvironmental changes and geochemistry of loesses and palaeosols in SE-Transdanubia, Hungary. Z. Geomorph. N. F., Suppl.-Bd., **110**: 69–83.

KABATA-PENDIAS A. and PENDIAS H. (1999) — Biogeochemia pierwiastków śladowych. Wydawnictwo Naukowe PWN, wyd. II zmienione. Warszawa.

KALINOVYCH N. (2002) — Plant cover in the Carpathians foreland (Ukraine) during the last Interglacial epoch (in Polish with English summary). In: Starsza i środkowa epoka kamienna w Karpatach (ed. J. Gancarski): 9–15. Muzeum Podkarpackie. Krosno.

KUSIAK J. (2007) — Controversies around TL dating of Late Pleistocene loess-palaeosol deposits at the Kolodiiv site (East Carpathian Foreland, Ukraine). Geol. Quart., **51**(2): 167–174.

ŁANCZONT M. and BOGUCKYJ A. (2002) — The examined loess sites in the Halyč Prydnistrov`ja region (in Polish with English summary). Stud. Geol. Pol., **119**: 33–181.

ŁANCZONT M. and BOGUCKYJ A. (2007) — High-resolution terrestrial archive of the climatic oscillation during Oxygen Isotope Stages 5–2 into loess-palaeosol sequence at Kolodiiv (East Carpathian Foreland, Ukraine). Geol. Quart., **51** (2): 105–126.

MADEYSKA T. (2002) — Loess and Palaeolithic of the Dniester River Basin, Halyč Region (Ukraine) (in Polish with English summary). Stud. Geol. Pol., **119**.

McLENNAN S. M. (1993) — Weathering and global denudation. J. Geol., **101**: 295–303.

MUNSELL SOIL COLOR CHARTS (1954). Baltimore.

NAWROCKI J., BOGUCKYJ A. and ŁANCZONT M. (2007) — Palaeomagnetic studies of the loess-palaeosol sequence from the Kolodiiv section (East Carpathian Foreland, Ukraine). Geol. Quart., **51** (2): 161–166.

PN–86/B–02480 — Grunty budowlane. Określenia, symbole, podział i opis gruntów.

ÖHLANDER B., THUNBERG J., LAND M., HÖGLUND L. O. and QUISHANG H. (2003) — Redistribution of trace metals in a mineralized spodsol due to weathering, Liikavaara, northern Sweden. Appl. Geochem., **18**: 883–899.

PEREDERIJ V. I. (2001) — Clay mineral composition and palaeoclimatic interpretation of the Pleistocene deposits of Ukraine. Quatern. Inter., **76/77**: 113–121.

RACINOWSKI R. (2002) — Heavy minerals of loess deposits in the Halyč Prydnistrov'ja region (in Polish with English summary). Stud. Geol. Pol., **119**: 219–236.

STERCKEMAN T., DOUAY F., BAIZE D., FOURRIER H., PROIX N. and SCHVARTZ C. (2004) — Factors affecting trace element concentrations in soils developed on recent marine deposits from northern France. Appl. Geochem., **19**: 89–103.

SYTNYK K., BEZUS'KO L., BEZUS'KO A. and BOZHKO Y. (2003) — Condition of palynological study of Riss-Würm deposits of section Kolodiiv (Ukraine, Ivano-Frankivska region). Biol. Ekol. Nauk. Zapys., **21**: 8–15.

WOLTHOORN A., TEMMINGHOFF E. J. M., WENG L. and VAN RIEMSDIJK W. H. (2004) — Colloid formation in groundwater: effect of phosphate, manganese, silicate and dissolved organic matter on the dynamic heterogeneous oxidation of ferrous iron. Appl. Geochem., **19**: 611–622.

YAKIMENKO E. Y. (1995) — Pleistocene palaeosols in the loess and loess-like sediments of the central part of the Russian Plain. Quatern. Sci. Rev., **14**: 747–753.

ZHANG Y. and FROST J. K. (2002) — Regional distribution of some elements in Illinois soils. Environ. Geol., **154**: 1–13. Illinois State Geol. Surv.